Kinetic Analysis of Terminal and Unactivated C−H Bond Oxyfunctionalization in Fatty Acid Methyl Esters by Monooxygenase-Based Whole-Cell Biocatalysis

Manfred Schrewe,[a] Anders O. Magnusson,[a,b] Christian Willrodt,[a] Bruno Bühler,[a,*] and Andreas Schmid[a]

[a] Laboratory of Chemical Biotechnology, Department of Biochemical and Chemical Engineering, TU Dortmund University, Emil-Figge-Str. 66, 44227 Dortmund, Germany
Fax: (+49)-231-755-7382; phone: (+49)-231-755-7384; e-mail: bruno.buehler@bci.tu-dortmund.de

[b] Current address: DECHEMA e.V., Bioverfahrenstechnik, Theodor-Heuss-Allee 25, 60486 Frankfurt/Main, Germany

Supporting information for this article is available on the WWW under http://dx.doi.org/10.1002/adcs.201100440.

Abstract: The alkane monooxygenase AlkBGT from *Pseudomonas putida* GPo1 constitutes a versatile enzyme system for the ω-oxyfunctionalization of medium chain-length alkanes. In this study, recombinant *Escherichia coli* W3110 expressing *alkBGT* was investigated as whole-cell catalyst for the regioselective biooxidation of fatty acid methyl esters to terminal alcohols. The ω-functionalized products are of general economic interest, serving as building blocks for polymer synthesis. The whole-cell catalysts proved to functionalize fatty acid methyl esters with a medium length alkyl chain specifically at the ω-position. The highest specific hydroxylation activity of $104\ U\,g_{CDW}^{-1}$ was obtained with nonanoic acid methyl ester as substrate using resting cells of *E. coli* W3110 (pBT10). In an optimized set-up, maximal 9-hydroxynonanoic acid methyl ester yields of 95% were achieved. For this specific substrate, apparent whole-cell kinetic parameters were determined with a V_{max} of $204\pm9\ U\,g_{CDW}^{-1}$, a substrate uptake constant (K_S) of $142\pm17\ \mu M$, and a specificity constant V_{max}/K_S of $1.4\ U\,g_{CDW}^{-1}\,\mu M^{-1}$ for the formation of the terminal alcohol. The same *E. coli* strain carrying additional *alk* genes showed a different substrate selectivity. A comparison of biocatalysis with whole cells and enriched enzyme preparations showed that both substrate availability and enzyme specificity control the efficiency of the whole-cell bioconversion of the longer and more hydrophobic substrate dodecanoic acid methyl ester. The efficient coupling of redox cofactor oxidation and product formation, as determined *in vitro*, combined with the high *in vivo* activities make *E. coli* W3110 (pBT10) a promising biocatalyst for the preparative synthesis of terminally functionalized fatty acid methyl esters.

Keywords: biotransformations; coupling efficiency; oxygenation; renewable resources; terminal functionalization; whole-cell biocatalysis

Introduction

Fatty acid methyl esters (FAMEs) constitute an interesting group of compounds, not only for energy storage (e.g., biodiesel) but also as a renewable feedstock for the chemical industry. FAMEs are produced by the transesterification of vegetable oils or waste lipids yielding glycerol as by-product.[1] *Via* oxyfunctionalization of the terminal alkyl carbons, FAMEs give access to bifunctional precursors for polymer synthesis. Unfortunately, the inert character of the sp^3 C−H bonds makes the alkyl chain of FAMEs barely accessible for specific oxyfunctionalization by chemical means. Multi-step processes including dehydrogenation, separation, and finally oxyfunctionalization are necessary to obtain the desired oxygenates.[2] Direct hydroxylation of sp^3 C−H bonds based on solid metal catalysts is a possible alternative.[3] The use of non-heme iron complexes was shown to allow the direct oxidation of C−H bonds under ambient conditions using H_2O_2 as oxidant.[4] However, application of these methods on a preparative scale is still hindered by poor selectivity, low turnover numbers, and the requirement for a large substrate surplus, in spite the progress concerning selectivity and predictability achieved by modifying the ligand frameworks of the
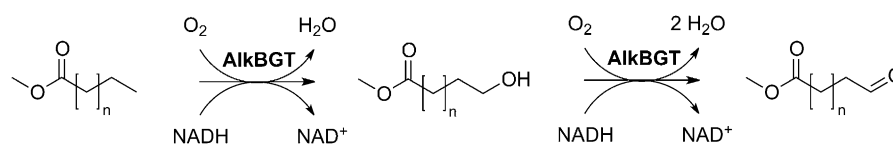
Figure 1. General scheme of the NADH-dependent terminal oxyfunctionalization of fatty acid methyl esters with the alkane monooxygenase system AlkBGT ($n = 2–9$).

catalytic complexes.[5] In general, chemical synthesis strategies and the application of metal catalysts are expensive and suffer from low efficiencies and poor selectivities.[6]

As a promising alternative, biocatalysts can be applied for the direct and selective oxyfunctionalization of inert C−H bonds.[7,8] Biocatalysts combine several desired characteristics for the efficient conversion of low-cost reactants to high-value products, such as high turnover numbers, high regio- and enantioselectivity, broad substrate spectrum, and environmentally friendly reaction conditions.[9] Among the enzymes catalyzing oxyfunctionalizations, oxygenases are most versatile with respect to the hydroxylation of sp^3 C−H bonds,[10] and are thus considered to have a great potential for application in industrial processes.[8,11] Iron-containing oxygenases are the most abundant and best investigated oxygenases catalyzing C−H oxyfunctionalizations.[10] For example, the hydroxylation of long chain fatty acids by the heme-containing cytochrome P450 BM3 is well investigated.[12,13] This enzyme features very high turnover numbers of up to $285 \, \text{s}^{-1}$ (determined based on the NADPH oxidation rate, frequently biased by uncoupling) but rather low regioselectivities by performing the reaction predominantly at three different subterminal positions.[13,14] Absolute regioselectivity could not be achieved by numerous attempts of protein engineering which, however, resulted in variants with increased regioselectivity.[15] In contrast, terminal oxyfunctionalization of long chain alkanes and fatty acids on a commercial scale is reported for *Candida tropicalis*.[16] Thereby, the initial hydroxylation is catalyzed by a cytochrome P450 monooxygenase coupled to an NADPH oxidoreductase.[17] Similarly, the alkane hydroxylase system AlkBGT from *Pseudomonas putida* GPo1 is known to catalyze oxyfunctionalizations of medium chain alkanes and fatty acids exclusively at terminal positions.[18,19] This three-component enzyme system consists of the monooxygenase (AlkB), a rubredoxin (AlkG), and a rubredoxin reductase (AlkT).[20,21] The latter two components are responsible for the electron transfer from NADH to AlkB. AlkB is a membrane-bound, non-heme diiron enzyme introducing one oxygen atom from molecular oxygen at the terminal position of alkanes. However, other aliphatic, alicyclic, and aromatic compounds are also accepted as substrates.[22] As proposed for oxygenases in general,

the use of whole cells is preferred over *in vitro* applications, because of the multi-component and partly membrane-bound nature of the enzyme complex, combined with the dependency on redox cofactors and a low stability of isolated enzymes.[23] In this study, aiming at the conversion of renewable feedstocks into products with added value, the use of recombinant *E. coli* containing AlkBGT was investigated for the selective formation of terminal alcohols and aldehydes from FAMEs (Figure 1). In order to identify possible implications of the whole-cell approach on substrate selectivity and availability/uptake, enriched and isolated enzyme preparations were investigated as well. Finally, coupling efficiencies of cofactor oxidation and FAME oxygenation were determined.

Results and Discussion

The ω-Oxyfunctionalization of FAMEs using *E. coli* W3110 Containing AlkBGT

FAMEs were tested as renewable substrates for terminal oxyfunctionalization by AlkBGT using resting, i.e., non-growing but metabolically active, cells of *E. coli* W3110 carrying the expression plasmid pGEc47. This plasmid encodes all genes of the alkane degradation pathway from *P. putida* GPo1.[19]

FAMEs ranging from pentanoic acid methyl ester to dodecanoic acid methyl ester were converted by resting cells of *E. coli* W3110 (pGEc47) (Figure 2). The alkane monooxygenase AlkBGT catalyzed the hydroxylation reaction exclusively at the ω-position leading to the formation of terminal alcohols, as verified by GC-MS (see the Supporting Information). In addition, small amounts of the corresponding aldehydes were detected as products of a second oxidation step, making up 0–7% of the total products. Only with hexanoic acid methyl ester as substrate, were equal amounts of alcohol and aldehyde formed. The highest specific hydroxylation activities were found for nonanoic and decanoic acid methyl ester conversions with 71 and 79 $U \, g_{CDW}^{-1}$, respectively. Hydroxylation activities of 31–37 $U \, g_{CDW}^{-1}$ were found for the conversion of octanoic, undecanoic, and dodecanoic acid methyl esters, whereas low activities of 2 and 4 $U \, g_{CDW}^{-1}$ were obtained for pentanoic and heptanoic
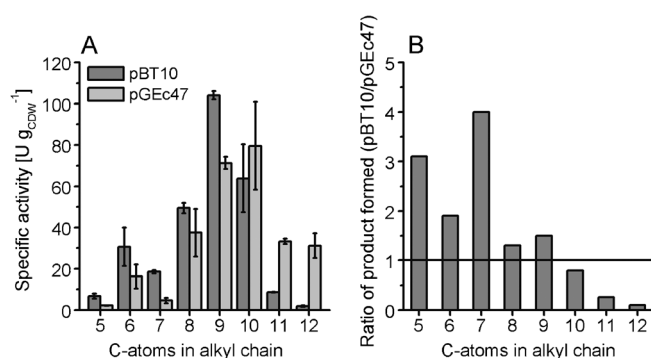
Figure 2. FAME spectrum for *in vivo* biocatalysis with AlkBGT. (**A**) Specific initial activities of resting cells of *E. coli* W3110 (pGEc47) (light grey) and *E. coli* W3110 (pBT10) (dark grey). (**B**) Ratios of product amounts formed with *E. coli* W3110 carrying pBT10 or pGEc47. Biomass conc.: ~1 $g_{CDW}L^{-1}$; substrate conc. 0.75–1.00 mM; each bar represents the average of at least two independent experiments.

Figure 3. SDS-PAGE analysis of the isolated total membrane fractions and of the supernatant after ultracentrifugation of cell extracts from (1) *E. coli* W3110, (2) *E. coli* W3110 (pGEc47), and (3) *E. coli* W3110 (pBT10). Arrow indicates AlkB (~41 kDa). Cells were grown at 30 °C in the presence of 0.5% (w/v) glucose and induced by addition of 0.025% (v/v) DCPK for 4 h.

acid methyl ester conversions, respectively. FAMEs can therefore be considered as highly suitable substrates for AlkBGT-containing recombinants. The maximum activities achieved were even higher than the 30–65 $U g_{CDW}^{-1}$ reported for *E. coli* W3110 (pGEc47) in conversions of octane and nonane.[22,24] In accordance with the reported values, octane and nonane were converted by *E. coli* W3110 (pGEc47) with initial activities of 64 and 59 $U g_{CDW}^{-1}$, respectively, in the set-up used in this study.

Plasmid pGEc47 encodes, next to the alkane monooxygenase system AlkBGT, also for an alcohol dehydrogenase (AlkJ), an aldehyde dehydrogenase (AlkH), and an acyl-CoA synthetase (AlkK).[25] The presence of the down-stream enzymes of the alkane degradation pathway in *E. coli* W3110 (pGEc47) might lead to product degradation thereby counteracting the desired product accumulation. *E. coli* species containing pGEc47ΔJ were shown to catabolize dodecanoic acid despite the presence of glucose.[26] Although alcohols and aldehydes were the only products detected during conversions of FAMEs in the performed short-term resting cell assays, possible utilization as carbon source *via* β-oxidation cannot be excluded and the presence of the down-stream enzymes should be avoided to increase product yields.

In order to obtain higher AlkBGT expression levels, resulting in higher specific activities and to avoid possible product degradation, the high-copy number plasmid pBT10 was constructed encoding only the three monooxygenase components. AlkB expression levels in *E. coli* W3110 (pGEc47) and *E. coli* W3110 (pBT10) were investigated by SDS-PAGE analysis of membrane fractions (Figure 3). AlkB was indeed more abundant in the membrane fraction of *E. coli* W3110 (pBT10), as compared to *E. coli*
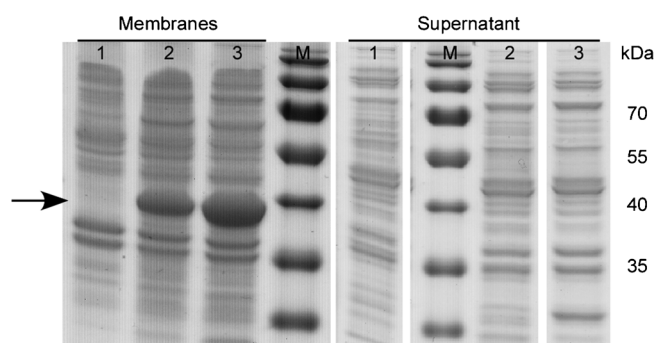
W3110 (pGEc47) representing approximately 60 and 20% of total membrane proteins 4 h after induction, respectively. After ultracentrifugation, no AlkB was observed in the supernatant. This indicates that all AlkB was incorporated into the cytoplasmic membrane. Inclusion body formation was not observed. Although not visible on SDS-PAGE gels, a similar increase in the expression levels can be assumed for *alkG* and *alkT* since the regulatory system and the gene order are identical in pBT10 and pGEc47.

E. coli W3110 (pBT10) showed significantly higher specific transformation rates (activities) for the smaller substrates with 5 to 9 carbon atoms in the alkyl chain, as compared to *E. coli* W3110 (pGEc47) (Figure 2). The highest specific activity of 104 $U g_{CDW}^{-1}$ was found for nonanoic acid methyl ester conversion. However, the longer and more hydrophobic substrates decanoic, undecanoic, and dodecanoic acid methyl esters were converted at higher rates by *E. coli* W3110 (pGEc47). *E. coli* W3110 (pBT10) showed specific dodecanoic acid methyl ester (DAME) hydroxylation rates of only 2%, as compared to nonanoic acid methyl ester (NAME) hydroxylation. This is in sharp contrast to the 43% observed with *E. coli* W3110 (pGEc47). Higher activities of *E. coli* W3110 (pBT10) towards the shorter substrates can be explained by higher AlkBGT levels in these cells, although the factor of activity increase varied between 1.3 and 4. However, catalytic activities for substrates with a longer alkyl chain did not correlate with AlkB expression levels.

The potential of the AlkBGT system for the production of terminal alcohols and the corresponding acids from alkanes has been reported previously.[27] Here, for the first time, AlkBGT is shown to be highly suitable for whole-cell conversions of renewa-

ble fatty acid methyl esters at high rates and with absolute terminal regioselectivity.

Conversion of FAMEs *in vitro*

Since AlkB expression levels cannot explain the low activities of *E. coli* W3110 (pBT10) towards the longer chain substrates, a component encoded on plasmid pGEc47 obviously facilitated their conversion. This can either be a protein assisting intracellular AlkB catalysis, in a similar way as reported for component B of the methane monooxygenase,[28] or a factor enhancing the intracellular availability of poorly water-soluble, larger substrates. In order to get more insight into the difference in substrate selectivity of the two recombinant strains, *in vitro* biotransformations of NAME and DAME were performed using isolated and enriched enzyme preparations. The enzyme preparations for AlkB and AlkG were obtained from different recombinant *E. coli* strains separately over-expressing the respective genes (see Experimental Section). The *in vitro* studies were performed by combining enriched AlkB and AlkG preparations and commercially available spinach reductase as described before.[20,22]

The background NADPH oxidation rates for incomplete reconstitutions were low, except for AlkG present together with the reductase, which showed increased background activities, probably caused by impurities of the AlkG preparation (Table 1). AlkG is known to transfer the electrons also to acceptors other than AlkB, for example, to cytochrome c.[29] The reconstituted three-component enzyme system showed significant NADPH consumption rates of $5.7 \, U \, L^{-1}$ without substrate addition. This implies the occurrence of uncoupling with electron transfer to molecular oxygen, typically resulting in the formation of reactive oxygen species, e.g., H_2O_2. Such reactions may also occur during biotransformation in the pres-

ence of substrate and product leading to uncoupling of cofactor consumption and product formation.

The maximal initial NADPH oxidation rates were 3- to 4-fold higher after addition of substrates compared to the background activity without substrate. Comparable NADPH consumption rates were found for substrate concentrations ranging from 500 to 2500 µM NAME and 200 to 1000 µM DAME. The addition of lower substrate concentrations led to lower specific NADPH oxidation rates, indicating kinetic substrate limitation. Since significant background NADPH oxidation rates were observed without the supply of FAMEs as substrate, not all reducing equivalents might have been used for product formation. Additionally, the presence of substrates and products might have induced uncoupling to occur at higher rates.[11,30] Therefore, NADPH consumption and product formation were compared over 15 min of reaction time (Table 2). Remarkably, the coupling efficiency was 100% using NAME as substrate, which implies that uncoupling could be avoided by addition of this substrate in non-limiting amounts. In contrast, the presence of DAME promoted uncoupling with slightly increasing coupling efficiencies with increasing substrate concentrations. The average coupling efficiency of 26% and the initial NADPH oxidation rate of

Table 2. Product formation and coupling efficiencies *in vitro*.

Substrate	$c_{substrate}$ [µM]	Product formed [µM][a]	NADPH consumed [µM][a]	Coupling efficiency [%]
NAME	500	194	194	100
	2500	203	204	100
DAME	200	52	216	24
	500	64	236	27
	1000	70	249	28

[a] Product formation and NADPH consumption was determined during 15 min of reaction.

Table 1. Initial NADPH consumption rates obtained for *in vitro* biotransformations of nonanoic acid methyl ester (NAME) and dodecanoic acid methyl ester (DAME).

Component	NADPH consumption rate $U \, L^{-1}$ [µmol min^{-1} L^{-1}]		
	Without substrate	NAME	DAME
AlkB	0.1	1.1[a]	n.d.[e]
AlkG	0.2	2.1[a]	n.d.[e]
Reductase (Red.)	0.1	0.7[a]	n.d.[e]
AlkB + AlkG	1.5	1.4[a]	n.d.[e]
AlkB + Red.	0.6	0.4[a]	n.d.[e]
AlkG + Red.	3.4	4.0[a]	n.d.[e]
AlkB + AlkG + Red.	5.7 ± 0.7 (71 ± 8)[d]	14.8 ± 0.1[b] (186 ± 1)[d]	22.1 ± 0.5[c] (276 ± 6)[d]

[a] 2.5 mM substrate added.
[b] Average for addition of 500, 1000, and 2500 µM substrate.
[c] Average for addition of 200, 500, and 1000 µM substrate.
[d] In brackets, rates are given as specific activities expressed in $U \, g_{AlkB}^{-1}$.
[e] n.d.: not determined.

Table 3. Comparison of specific activities obtained for nonanoic acid methyl ester (NAME) and dodecanoic acid methyl ester (DAME) conversions *in vivo* and *in vitro*.

System	Substrate	Specific activity [$U g^{-1}$]	Ratio activities NAME/DAME
E. coli W3110 (pBT10)	NAME	104 ± 2[a]	55
	DAME	1.9 ± 0.4[a]	
E. coli W3110 (pGEc47)	NAME	71 ± 3[a]	2.3
	DAME	31 ± 6[a]	
in vitro	NAME	186 ± 1[b]	2.6
	DAME	72 ± 2[c]	

[a] $U g_{CDW}^{-1}$.
[b] $U g_{AlkB}^{-1}$; based on initial NADPH oxidation activities assuming 100% coupling.
[c] $U g_{AlkB}^{-1}$; based on initial NADPH oxidation activities assuming 26% coupling.

$22.1 \, U L^{-1}$ (Table 1) translate into $16.4 \, U L^{-1}$ of uncoupled NADPH oxidation in the presence of DAME, which is a factor of 3 higher than the uncoupling observed in the absence of DAME. Obviously, DAME addition led to a significant acceleration of uncoupling reactions *in vitro*.

In an analogous *in vitro* set-up similarly high NADPH oxidation rates have been observed for the hydroxylation of C_8–C_{12} alkanes by AlkBGT, whereas *Pseudomonas* cells showed decreasing product formation rates with increasing chain length (being maximal for C_8 and C_9 and not detectable for C_{12}).[22] Grant et al. showed that *E. coli* DH1 (pGEc47ΔJ) containing AlkBGT preferred the oxidation of octane over dodecane. Dodecane oxidation rates constituted only 14–16% of octane oxidation rates.[26] This discrepancy between *in vitro* NADPH oxidation and *in vivo* product formation may, at least in part, be attributed to uncoupling in the presence of long chain substrates as was the case for FAMEs. However, mass transfer limitations also may reduce *in vivo* conversion rates of long chain substrates such as dodecane.

Van Beilen, Witholt, and co-workers reported increased growth rates on longer chain alkanes (C_{12} to C_{16}) for recombinant *Pseudomonas* strains with mutant *alkB* genes.[31] It was concluded that the exchange of the bulky tryptophan residue with the smaller amino acids cysteine or serine (W55C and W55S) enlarged the substrate binding pocket and thus enabled larger substrate molecules to access the enzyme with reduced steric hindrance. Since uncoupling is described for substrates not fitting well into the active site of an enzyme,[32] the described mutations might have led to an improved coupling efficiency, higher alkane conversion rates, and subsequently to higher growth rates.

In order to compare the obtained *in vitro* and *in vivo* results, the initial *in vitro* NAME and DAME hydroxylation rates were calculated from the NADPH oxidation rates assuming 100 and 26% coupling, respectively (Table 3). Interestingly, the ratio of initial NAME and DAME hydroxylation rates observed in the reconstituted enzyme assays correlated with the ratio observed with *E. coli* W3110 (pGEc47). In contrast, *E. coli* W3110 (pBT10) showed a much higher ratio. This and the fact that the enzyme preparations were obtained from strains over-expressing *alkB* or *alkG* only, indicate that pGEc47 does not encode components supporting the AlkBGT-catalyzed conversion of DAME but rather improves intracellular substrate availability. As the outer membrane of Gram-negative bacteria constitutes an effective barrier for large and hydrophobic compounds,[33] whole-cell bioconversions of such substrates are often limited by poor substrate availability in the bacterial cell.[11,34] In cells containing pGEc47, DAME mass transfer over the outer membrane may be facilitated by the pGEc47-encoded outer membrane protein AlkL, which has been hypothesized to be involved in substrate uptake.[25]

A comparison of the whole-cell activities with *in vitro* results obtained for FAME conversion revealed limitations for the larger and more hydrophobic substrate DAME to occur on both levels, the selectivity of the monooxygenase AlkB and, for *E. coli* W3110 (pBT10), intracellular substrate availability.

NAME was found to be a preferred substrate for terminal oxyfunctionalization by AlkBGT both in terms of coupling and whole-cell activity. To the best of our knowledge, $104 \, U g_{CDW}^{-1}$, as determined here, is the highest whole-cell activity reported for AlkBGT to date.

Characterization of *E. coli* W3110 (pBT10) as Catalyst for NAME Oxyfunctionalization

To determine apparent whole-cell kinetics, resting cell assays with varying NAME and 9-hydroxynonanoic acid methyl ester (HNAME) concentrations were performed. Alcohol conversion was investigated because low aldehyde concentrations have been found in initial experiments. The conversions of both substrates followed Michaelis–Menten-like kinetics (Figure 4).
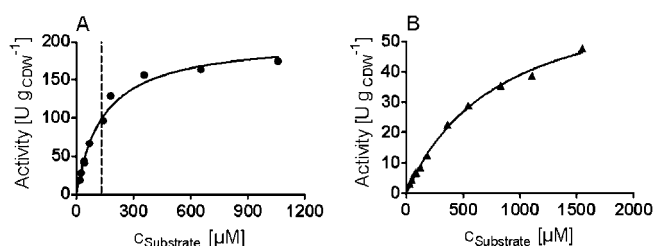
Figure 4. Apparent Michaelis–Menten-like kinetics for whole-cell conversions of (**A**) nonanoic acid methyl ester (NAME) (dashed line represents the NAME solubility of 133 μM in water) and (**B**) 9-hydroxynonanoic acid methyl ester (HNAME) catalyzed by *E. coli* W3110 (pBT10). Initial activities determined within 5 min of biotransformation are given applying a biomass concentration of $0.08\ g_{CDW}\,L^{-1}$.

Even with NAME concentrations exceeding the solubility limit of 133 μM in water, the kinetics followed Michaelis–Menten-like behaviour (Figure 4, **A**).

Considering apparent kinetic parameters (Table 4), the initial hydroxylation step is preferred over alcohol oxidation. Thereby, NAME hydroxylation catalyzed by *E. coli* W3110 (pBT10) shows an efficiency which is comparable to styrene epoxidation by recombinant *E. coli* containing the styrene monooxygenase StyAB ($V_{max} = 107\ U\,g_{CDW}^{-1}$; $K_S = 64$ μM)[35] and pseudocumene hydroxylation by *E. coli* containing the xylene monooxygenase XylMA ($V_{max} = 351\ U\,g_{CDW}^{-1}$; $K_S = 202$ μM),[36] two of the most efficient biocatalytic whole-cell oxyfunctionalization reactions reported.

Optimization of Nonanoic Acid Methyl Ester Oxyfunctionalization

In order to optimize product yields, NAME was added in concentrations varying from 1 to 10 mM to resting *E. coli* W3110 (pBT10) and the time course of the biotransformation was followed. In all cases, the terminal alcohol was the main product accumulating, with up to 0.3 mM of the aldehyde as minor by-product (Figure 5, **A–D**). The addition of 5.1 mM substrate appeared to be optimal. 4.8 mM substrate were converted within 2 h of reaction time resulting in alcohol and aldehyde concentrations of 4.5 and 0.2 mM, respectively. The product concentrations correlated to yields based on consumed substrate of 95 and 4% for alcohol and aldehyde, respectively (Table 5).
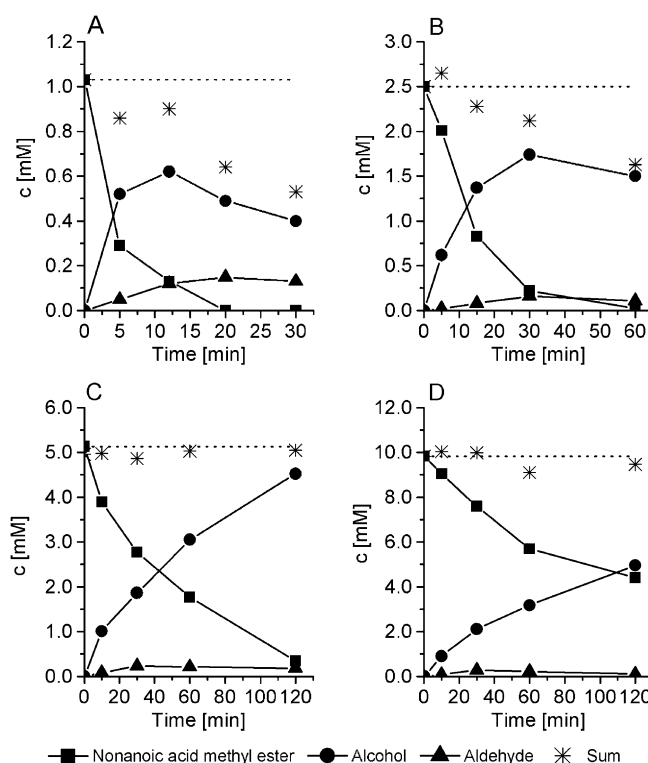

— Nonanoic acid methyl ester   —●— Alcohol   —▲— Aldehyde   ✳ Sum

Figure 5. Biotransformation of 1.0, 2.5, 5.1, and 9.8 mM of NAME with resting *E. coli* W3110 (pBT10). Dashed line represents the initial substrate concentration. A biomass concentration of $1.2\ g_{CDW}\,L^{-1}$ was applied.

The maximum specific activities reached in the three biotransformations with initial substrate concentrations of 2.5, 5.1, and 9.8 mM were on the expected level of $100\ U\,g_{CDW}^{-1}$ as seen in previous experiments, whereas the addition of 1 mM substrate led to substrate limitation (Table 5).

After the first 10 min of the biotransformations with 5.1 and 9.8 mM NAME, approximately 1 mM of HNAME was produced (Figure 5, **C** and **D**). Using the Michaelis–Menten equation and the determined apparent kinetic parameters (Table 4), specific alcohol oxidation rates of $39\ U\,g_{CDW}^{-1}$ would be expected with 1 mM of the alcohol present. However, the maximum alcohol oxidation activities observed in these experiments were only $8\ U\,g_{CDW}^{-1}$. This indicates that the alcohol lost the competition for the catalyst against NAME, which is in accordance with its significantly higher substrate uptake constant as compared to NAME (Table 4). Similar results have been published

Table 4. Apparent kinetic parameters for the whole-cell conversions of nonanoic acid methyl ester (NAME) and 9-hydroxynonanoic acid methyl ester (HNAME) with resting *E. coli* W3110 (pBT10).

Substrate	Apparent V_{max} [$U\,g_{CDW}^{-1}$]	Apparent K_S [μM]	V_{max}/K_S [$U\,g_{CDW}^{-1}\,μM^{-1}$]
NAME	204 ± 9	142 ± 17	1.4
HNAME	71 ± 3	823 ± 70	0.1

Table 5. Maximum specific activities and yields obtained in bioconversions with different initial NAME concentrations.

Time [min]	Initial substrate conc. [mM]	Remaining substrate [%]	Max. NAME oxidation rate [U g_{CDW}^{-1}]	Max. HNAME oxidation rate [U g_{CDW}^{-1}]	Y alcohol [%][a]	Y aldehyde [%][a]	Y oxidation products [%][a]
12	1.0	13	83	8	69	13	82
30	2.5	9	100	5	76	7	83
120	5.1	7	103	8	95	4	99
120	9.8	45	96	8	92	2	94

[a] Yields were calculated based on converted substrate.

recently for octane conversions by recombinant *E. coli* expressing *alkBGT*,[26] and for xylene monooxygenase containing *E. coli* converting pseudocumene and toluene.[36] Alcohol oxidation was slow as long as the initial substrate was present in excess and the alcohol concentration was below a critical limit.

During biotransformations with initial substrate concentrations of 1 and 2.5 mM, alcohol and aldehyde concentrations decreased once NAME was almost depleted (Figure 5, **A** and **B**). This and the decrease in total substrate and product recovery indicate product degradation. If product degradation led to the formation of molecules carrying a carboxyl group (either by ester hydrolysis or by formation of nonanedioic acid monomethyl ester), these molecules could enter the β-oxidation cycle. Product degradation can be caused by host intrinsic enzymes as reported by Meyer et al. for *m*-nitrotoluene and its oxidized derivatives,[37] or by the overoxidation of the products catalyzed by AlkBGT. Overoxidation is a feature often observed for monooxygenases.[11] For xylene monooxygenase XylM from *P. putida* mt-2 with a sequence identity of 25% to AlkB,[38] the overoxidation of toluene to benzoic acid was reported.[39] Here, the occurrence of AlkBGT-catalyzed overoxidation seemed to be the dominant effect since no further degradation was observed as long as the NAME concentration was not limiting (Figure 5, **C** and **D**).

The obtained maximal hydroxylation activities of approximately 100 U g_{CDW}^{-1} at biomass concentrations of 1.2 $g_{CDW}L^{-1}$ (Table 5) were significantly lower than the activities observed during kinetic analyses. Applying very low biomass concentrations of 0.08 $g_{CDW}L^{-1}$, maximal specific activities of 175 U g_{CDW}^{-1} were determined (Figure 4). In order to investigate the influence of the biomass concentration on the specific activity, biotransformations with varying cell concentrations were perfomed. Volumetric activities correlated linearly with biomass concentrations up to 1.3 $g_{CDW}L^{-1}$ reaching a plateau with higher biomass concentrations (Figure 6). Mass transfer limitations of either substrate or oxygen probably caused this effect.

The corresponding specific activities observed can be divided into three different stages (Figure 6). For an aqueous substrate concentration corresponding to the solubility limit of 133 μM, 100 U g_{CDW}^{-1} can be ex-
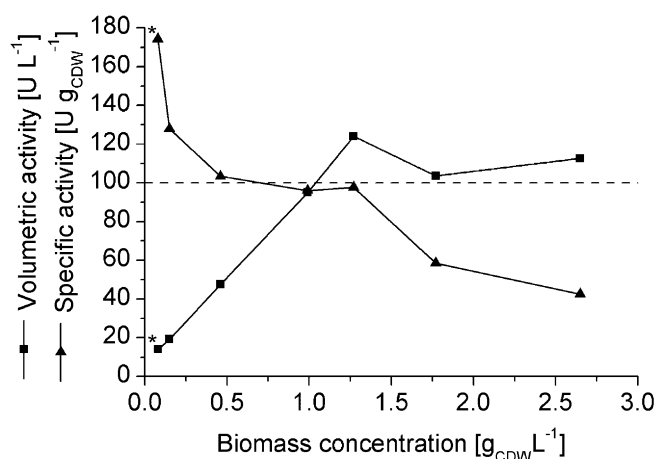

Figure 6. Initial volumetric and specific NAME oxyfunctionalization activities of resting *E. coli* W3110 (pBT10) as a function of biomass concentration. The dashed line represents the expected specific activity according to the kinetics determined for NAME conversion (Figure 4 **A**) using its solubility limit of 133 μM in water as substrate concentration. A substrate concentration of 2.5 mM was applied. * Only 1 mM of substrate was added (data from kinetic assay).

pected considering the kinetics for NAME conversion (Figure 4, Table 4). For biomass concentrations between 0.5 and 1.3 $g_{CDW}L^{-1}$, activities were found to be in this range. The application of lower biomass concentrations (0.08 and 0.16 $g_{CDW}L^{-1}$) resulted in significantly higher specific activities. Direct substrate uptake from organic phase droplets (undissolved substrate) could be a possible explanation for these high conversion rates. Such direct uptake is considered to be one of the mechanisms how hydrocarbon degraders get access to poorly water soluble substrates.[40] Bacterial cells collide with and/or attach to these droplets and thereby face far higher substrate concentrations as present in the aqueous surrounding. The addition of 2.5 mM NAME and mixing on an orbital shaker is expected to result in the formation of substrate droplets in the aqueous phase. Whereas such direct uptake may have occurred in experiments with very low biomass concentrations, direct access to a substrate droplet may decrease with increasing biomass concentrations. At cell concentrations above 1.3 $g_{CDW}L^{-1}$ in the set-up used, oxygen mass transfer

over the gas/liquid phase boundary and/or substrate mass transfer over the organic/aqueous phase boundary may have become limiting, resulting in decreased specific activities. However, such mass transfer can significantly be improved by the use of standard bioreactor configurations, e.g., stirred tank reactors, making the use of high cell densities feasible for biocatalytic NAME hydroxylation.

Conclusions

This study showed the high potential of the whole-cell biocatalyst *E. coli* W3110 (pBT10) expressing the alkane monooxygenase genes *alkBGT* for the specific ω-oxyfunctionalization of medium chain length FAMEs as renewable feedstocks. It also demonstrated the control of catalyst efficiency by various parameters other than enzyme characteristics. The exclusive formation of terminally functionalized products from unactivated alkyl carbons and the high hydroxylation rates achieved with AlkBGT *in vivo*, ranging among the highest oxyfunctionalization rates reported for whole-cell biocatalysis, underline the versatility of this enzyme system. The efficient coupling of cofactor consumption and product formation (100%), the high alcohol yield (95%), and the high conversion rate (104 U g$_{CDW}^{-1}$) achieved with the substrate nonanoic acid methyl ester offer an excellent starting point for the preparative synthesis of terminally functionalized FAMEs in a biotransformation process. Beside substrate selectivity of AlkBGT, substrate availability and uncoupling appeared to be critical for the conversion of longer and more hydrophobic substrates, of which the intracellular availability was higher in *E.*

coli W3110 (pEGc47) expressing all genes of the alkane degradation pathway of *P. putida* GPo1. This points to the presence of a specific substrate uptake system in the latter strain. Next to substrate availability, substrate selectivity and coupling efficiency of the AlkBGT enzyme complex are engineering targets to improve the ω-oxyfunctionalization of longer chain FAMEs.

Experimental Section

Chemical, Bacterial Strains, and Media

All chemicals used for this study were purchased from Sigma–Aldrich (Steinheim, Germany) or Carl Roth (Karlsruhe, Germany) with the highest purity available except for 9-hydroxynonanoic acid methyl ester (purity of ≥95%, TCI Europe N.V., Zwijndrecht, Belgium) and 12-hydroxydodecanoic acid methyl ester (purity of ≥95%, Evonik Degussa GmbH, Marl, Germany). All strains and plasmids used in this study are listed in Table 6. For cloning purposes, *E. coli* DH5α was used. For expression and biotransformation experiments *E. coli* W3110 was transformed with the different plasmids. Strains were cultivated in M9[41] or modified M9 (M9*)[42] medium supplemented with 1 mL L^{-1} US^{Fe} trace element solution[43] and 0.5% (w/v) glucose or in LB medium.[41] The antibiotics (50 mg L^{-1} kanamycin or 12.5 mg L^{-1} tetracycline) were added to all media if appropriate. Solid media contained 15 g L^{-1} agar.

DNA Manipulation Techniques

Standard techniques were used for restriction analysis, cloning, and agarose gel electrophoresis.[41] Phusion High-Fidelity DNA Polymerase obtained from Finnzymes Oy (Espoo, Finland) was used for all PCR reactions. All restriction endonucleases were purchased from Fermentas GmbH (St.

Table 6. Bacterial strains and plasmids used in this study.

Strain or Plasmid	Characteristics	Ref.
Strain		
E. coli DH5α	*sup*E44 Δ*lac*U169 (Φ80 *lac*ZΔM15) *hsd*R17 *rec*A1 *end*A1 *gyr*A96 *thi*-1 *rel*A1	[44]
E. coli W3110	F$^-$, λ^{-1}, *rph*-1, *IN*(*rrnD-rrnE*)1	[45]
Plasmid		
pCOM10	alkane responsive broad-host-range vector; P$_{alkB}$; *alkS*	[46]
pSMART-HCKan	blunt-end subcloning vector, Km^r	Lucigen Corporation (Middleton, WI, USA)
pGEc47	contains genes necessary for growth on alkanes (*alkBFGHJKL* and *alkST*) in broad-host-range vector pLAFR1, Tc^r	[19]
pSMART-BFG	pSMART-HCKan containing *alkBFG*	this study
pSMART-T	pSMART-HCKan containing *alkT*	this study
pBG10	pCOM10 containing *alkBFG*	this study
pBT10	contains genes for alkane monooxygenase (*alkBFG* and *alkST*) in broad-host range vector pCOM10, Km^r	this study
pAMB	contains gene for the oxygenase component *alkB* in broad-host range vector pCOM10, Km^r	this study
pAMG	contains gene for the rubredoxin *alkG* in broad-host range vector pCOM10, Km^r	this study

Leon-Rot, Germany). All primers were purchased from Eurofins MWG (Ebersberg, Germany). Successful cloning was confirmed by sequencing by Eurofins MWG.

A two-step cloning strategy was followed to obtain an *alkBGT* expression vector with a gene organization closely related to the original operons in *P. putida* GPo1. The *alkBFG* genes were amplified by PCR from plasmid pGEc47[19] using the primers 5′-AAGGGAATTC<u>CATATG</u>CTT GAGAAACACAGAGTTC-3′ containing an *Nde*I restriction site (underlined) and 5′-AAAATTCGC<u>GTCGAC</u>AAGCGCTGAATGGG TATCGG-3′ containing a *Sal*I restriction site (underlined). The PCR product was cloned into the blunt-end cloning vector pSMART-HCKan (Lucigen Corporation, Middleton, WI, USA) giving pSMART-BFG. After restriction with *Nde*I and *Sal*I, the fragment obtained was ligated into the alkane responsive broad-host-range expression vector pCOM10[46] cut with the same enzymes resulting in the formation of plasmid pBG10 containing *alkBFG* under control of the P_{alkB} promoter.

The *alkT* gene was amplified from plasmid pGEc47 by PCR using the primers 5′-TGAGACAGTGGCTGTTAGAG-3′ and 5′-TAATAACCG<u>CTCGAG</u>AACGCTTACCGCCAACACAG-3′ containing an *Xho*I restriction site (underlined). The PCR product was cloned into pSMART-HCKan giving pSMART-T. After restriction with *Pac*I and *Xho*I, the fragment obtained was ligated into pBG10 cut with the same restriction enzymes. The resulting plasmid pBT10 contained *alkT* under the control of P_{alkS} downstream of the *alkS* gene.

Plasmids for separate *alkB* and *alkG* expression were constructed to facilitate the enrichment of single enzyme components for *in vitro* studies. Both genes were amplified from pBT10 using for *alkB* the primers 5′-GAGAATTC<u>CATATG</u>CTT GAGA-3′ containing a *Nde*I restriction site (underlined) and 5′-GCTGGA<u>AGATCT</u>ACGATGCTACCGCAGAG-3′ containing a *Bgl*II restriction site (underlined) and, for *alkG*, the primers 5′-GGGAATTC<u>CATATG</u>GCTAGCTATAAATGCCC-3′ containing a *Nde*I restriction site (underlined) and 5′-TTACGC<u>GGATCCT</u>CACTTTTCCTCGTAGAGCA-3′ containing a *Bam*HI restriction site (underlined). The PCR products were cut with the respective restriction enzymes and separately ligated into pCOM10[46] cut with *Nde*I and *Bam*HI resulting in pAMB and pAMG, carrying the *alkB* and *alkG* genes, respectively, under control of the P_{alkB} promoter.

Cultivation and Gene Expression

Cultivation was generally performed in orbital shakers (Multitron, Infors HT, Bottmingen, Switzerland) at 200 rpm and 37 °C for LB cultures or 30 °C for minimal medium cultures. Precultures of 5 mL LB medium were inoculated with a single colony of the recombinant *E. coli* strain and grown for 10 h. Subsequently, 500 μL of the precultures were used to inoculate 50 mL M9* medium. These cultures were incubated overnight and used either to inoculate a bioreactor (see below) or 100 mL M9* shake flask cultures to an initial biomass concentration of 0.03 $g_{CDW}L^{-1}$. The cultures were incubated until a biomass concentration of 0.08 $g_{CDW}L^{-1}$ was reached. Then, *alkBGT* expression was induced by the addition of 0.025% (v/v) dicyclopropyl ketone (DCPK) and the cells were incubated for another 4 h. Subsequently, the AlkBGT-containing cells were harvested by centrifugation (4595 *g*, 10 min, 4 °C).

M9* precultures of recombinant *E. coli* W3110 carrying pAMB or pAMG were used to inoculate a bioreactor (KLF 2000, Bioengineering AG, Wald, Switzerland) with 1.5 L of M9 medium containing 3% (w/v) glucose. The dissolved oxygen tension (DOT) was determined with an autoclavable amperometric probe (Mettler–Toledo GmbH, Schwerzenbach, Switzerland) and the pH (pH probe: Mettler–Toledo GmbH, Schwerzenbach, Switzerland) was automatically kept at 7.2 by adding 30% phosphoric acid and 25% NH$_4$OH. Temperature, agitation frequency, and aeration rate were maintained at 30 °C, 1.5 Lmin^{-1}, and 1500 rpm, respectively. After batch phase, 0.4% (v/v) US^{Fe} trace solution were added to the cells and an exponential feed [50% (w/v) glucose, 13.7 gL^{-1} magnesium sulfate] was started for a glucose limited exponential growth rate μ=0.2 h^{-1}. After 3–4 h of exponential growth, *alk*-gene expression was induced by addition of 0.025% (v/v) DCPK and after another 4 h of fed-batch cultivation, the cells were harvested by centrifugation, washed with 10 mM TRIS-HCl (pH 8.0) for AlkB enrichment or 50 mM TRIS-HCl (pH 7.5) for AlkG enrichment, and stored as pellet at −20 °C or immediately used for protein enrichment.

Protein Isolation and Enrichment

For isolation of total membrane fractions from *alkBGT* expressing strains, cell pellets were resuspended in a 55 mM sodium-potassium phosphate buffer (pH 7.5) and disrupted by two passages through a French press (5.5 MPa, SLM-Aminco, Rochester, NY, USA). Cell debris was removed by centrifugation at 12,000 *g* and 4 °C for 15 min. The supernatant was centrifuged at 200,000 *g* and 4 °C for 2 h. The resulting pellet containing the membrane fraction was resuspended in the same buffer and analyzed by SDS-PAGE.

For AlkB enrichment, spheroplasting was performed as described previously,[47] with the modification that no EDTA was added as it is known to impair AlkB activity.[48] The resulting pellet was stored at −20 °C. For further purification, the pellet was resuspended in 10 mM TRIS-HCl (pH 8.0) to a concentration corresponding to 25 $g_{CDW}L^{-1}$. Bacterial DNA was degraded by adding 5 mM magnesium sulphate and 0.25 UmL^{-1} DNase, and incubation on ice for 20 min. Then, the solution was slowly passed through a French press. Cell debris was removed by centrifugation at 12,000 *g* and 4 °C for 30 min. The supernatant was centrifuged at 250,000 *g* and 4 °C for 90 min. The pellet from the ultracentrifugation was directly used or stored at −20 °C until needed. AlkB was enriched by density gradient centrifugation. A discontinuous sucrose gradient was prepared ranging from 30–55% (w/v) sucrose, with steps of 5% sucrose. Each density fraction had a volume of 1.76 mL except the 30% fraction, which had a volume of 0.88 mL. The pellet obtained by ultracentrifugation was dissolved in 25% sucrose and 0.8 mL of this solution was loaded on top of the gradient. Thus, the total volume in each centrifugation tube was 10.5 mL. After centrifugation at 170,000 *g* and 4 °C for 22 h, the solution was fractionized by carefully pipetting the sucrose gradient from the top. After analyzing the different fractions by SDS-PAGE, the AlkB containing fractions were pooled and stored at −20 °C. The yield was 15% and purity was estimated by SDS-PAGE to be over 80%.

For AlkG enrichment, cells were resuspended in 50 mM TRIS-HCl (pH 7.5) to a density of 40 $g_{CDW} L^{-1}$ and disrupted by 5 sequential French press passages. After removal of cell debris by centrifugation at 4595 g and 4°C for 30 min, the supernatant was incubated at 70°C for 15 min and then centrifuged at 12,000 g and 4°C for 10 min to remove heat-denatured proteins. An ice-cold and saturated ammonium sulphate solution was added dropwise to the supernatant under slow stirring in an ice-bath. The fraction between 30% and 60% saturation was collected and stored at −20°C until used. The AlkG preparation had a purity of 50% as determined by SDS-PAGE.

Sodium dodecyl sulphate-polyacrylamide gel electrophoresis (SDS-PAGE) was performed by the method of Laemmli.[49] Gels were stained with Coomassie blue. A molecular weight standard (Fermentas SM0671) was used as reference.

Biotransformations

The AlkBGT activity of resting cells was determined using cells resuspended in 1 mL of 50 mM potassium phosphate buffer (pH 7.4) containing 1% (w/v) glucose at a determined cell density between 0.08 and 2.7 $g_{CDW} L^{-1}$. The reaction mixtures were incubated for 5 min at 30°C in an orbital shaker (300 min^{-1}) in order to adapt to the reaction conditions. All assays contained 2.5% (v/v) ethanol after addition of the substrate stock solution. The reactions were started by addition of substrate solution and stopped after different time intervals by addition of 1 mL ice-cold diethyl ether containing dodecane (0.2 mM) as internal standard for gas chromatography (GC) analysis. Extraction was performed by vortexing the sample for 1 min. Subsequently, the samples were centrifuged (4595 g, 4°C, 5 min) for improved phase separation, the ether phase was dried over anhydrous Na_2SO_4, and analyzed by GC. One unit (U) of whole-cell activity was defined as 1 µmol of product being produced per minute. Specific activities ($U g_{CDW}^{-1}$) were calculated per gram cell dry weight (CDW).

In vitro activity assays with a reconstituted enzyme system with enriched AlkB and AlkG enzyme preparations were performed essentially as described earlier.[22] The reaction volume was 1 mL and contained 80 µg AlkB, 400 µg AlkG, 80 mU spinnach ferredoxin reductase, 300 µM NADPH, 0.2 to 2.5 mM substrate, 1% acetone, and 50 mM TRIS-HCl (pH 7.5). All components except for the substrate and acetone were mixed in a cuvette and tempered at 30°C. The reaction was started by the addition of nonanoic acid methyl ester or dodecanoic acid methyl ester dissolved in acetone followed by short mixing. The consumption of NADPH was followed by measuring the decrease in absorption at 340 nm. After 15 min, the reaction was stopped by extracting the remaining substrate and products formed with an equal volume of ethyl acetate containing 0.5 mM decane as internal standard for GC analysis. The product concentration was determined by GC-analysis. AlkB was applied as the rate-limiting component. The extraction efficiency for nonanoic and dodecanoic acid methyl ester and the corresponding products was determined with known amounts of the compounds added to the assay solution containing all the components.

Analytical Methods

FAMEs and corresponding products were quantified by GC (Trace GC UltraTM, ThermoFisher Scientific, Waltham, USA) equipped with a FactorFour-VF-5 ms capillary column, containing 5% phenyl- and 95% dimethylpolysiloxane (30 m, ID 0.25 mm, DF 0.25 µm, Varian, Palo Alto, California, USA) with molecular nitrogen as carrier gas. Detection was accomplished by an FID. For pentanoic and hexanoic acid methyl esters the temperature profile was (i) 40°C for 3 min, (ii) 40 to 170°C at 15°C min^{-1}, (iii) 170 to 300°C at 100°C min^{-1}, and (iv) 300°C for 3 min. For all other FAMEs the temperature profile was (i) 80 to 280°C at 15°C min^{-1}; (ii) 280 to 300°C at 100°C min^{-1}, and (iii) 2.5 min at 300°C. Products were quantified based on standard calibration curves for available standards. Concentrations of non-available compounds were estimated based on their carbon content, comparison with the available standards (9-hydroxynonanoic and 12-hydroxydodecanoic acid methyl ester), as well as from substrate depletion.

The products of FAME conversions were identified by gas chromatography mass spectrometry (GC-MS) using a Varian 1200 Quadrupole MS coupled to a Varian CP-3800 Gas Chromatograph using helium as carrier. The same column and temperature profiles as used for GC-FID analysis were applied. The oxyfunctionalized products were identified by their characteristic MS fragmentation patterns.

Acknowledgements

References

[1] a) D. Y. C. Leung, X. Wu, M. K. H. Leung, *Appl. Energy* **2010**, *87*, 1083–1095; b) A. Y. Tremblay, P. G. Cao, M. A. Dube, *Energy Fuels* **2008**, *22*, 2748–2755.

[2] J. A. Labinger, J. E. Bercaw, *Nature* **2002**, *417*, 507–514.

[3] R. Burch, M. J. Hayes, *J. Mol. Catal. A: Chem.* **1995**, *100*, 13–33.

[4] a) F. Gozzo, *J. Mol. Catal. A: Chem.* **2001**, *171*, 1–22; b) A. A. Fokin, P. R. Schreiner, *Adv. Synth. Catal.* **2003**, *345*, 1035–1052.

[5] a) M. S. Chen, M. C. White, *Science* **2007**, *318*, 783–787; b) M. S. Chen, M. C. White, *Science* **2010**, *327*, 566–571.

[6] a) R. A. Periana, G. Bhalla, W. J. Tenn, K. J. H. Young, X. Y. Liu, O. Mironov, C. J. Jones, V. R. Ziatdinov, *J. Mol. Catal. A: Chem.* **2004**, *220*, 7–25; b) E. E. Wolf, *Methane conversion by oxidative processes*, Van Nostrand Reinhold, New York, **1992**.

[7] a) W. A. Duetz, J. B. van Beilen, B. Witholt, *Curr. Opin. Biotechnol.* **2001**, *12*, 419–425; b) J. B. van Beilen, E. G. Funhoff, *Curr. Opin. Biotechnol.* **2005**, *16*, 308–314; c) S. F. Ye, F. Neese, *Curr. Opin. Chem. Biol.* **2009**, *13*, 89–98.

[8] B. Bühler, A. Schmid, *J. Biotechnol.* **2004**, *113*, 183–210.

[9] S. M. Resnick, K. Lee, D. T. Gibson, *J. Ind. Microbiol. Biotechnol.* **1996**, *17*, 438–457.

[10] B. Bühler, A. Schmid, *Selective enzymatic hydroxylations*, in: Handbook of *C−H Transformations*, (Ed.: G. Dyker), Vol. 2. Wiley-VCH, Weinheim, **2005**, pp 516–529.

[11] J. B. van Beilen, W. A. Duetz, A. Schmid, B. Witholt, *Trends Biotechnol.* **2003**, *21*, 170–177.

[12] a) S. N. Daff, S. K. Chapman, K. L. Turner, R. A. Holt, S. Govindaraj, T. L. Poulos, A. W. Munro, *Biochemistry* **1997**, *36*, 13816–13823; b) A. W. Munro, D. G. Leys, K. J. McLean, K. R. Marshall, T. W. B. Ost, S. Daff, C. S. Miles, S. K. Chapman, D. A. Lysek, C. C. Moser, C. C. Page, P. L. Dutton, *Trends Biochem. Sci.* **2002**, *27*, 250–257; c) Y. Miura, A. J. Fulco, *Biochim. Biophys. Acta* **1975**, *388*, 305–317.

[13] M. A. Noble, C. S. Miles, S. K. Chapman, D. A. Lysek, A. C. Mackay, G. A. Reid, R. P. Hanzlik, A. W. Munro, *Biochem. J.* **1999**, *339*, 371–379.

[14] a) P. P. Ho, A. J. Fulco, *Biochim. Biophys. Acta* **1976**, *431*, 249–256; b) L. O. Narhi, A. J. Fulco, *J. Biol. Chem.* **1986**, *261*, 7160–7169; c) N. Shirane, Z. H. Sui, J. A. Peterson, P. R. O. Demontellano, *Biochemistry* **1993**, *32*, 13732–13741; d) A. J. Warman, O. Roitel, R. Neeli, H. M. Girvan, H. E. Seward, S. A. Murray, K. J. McLean, M. G. Joyce, H. Toogood, R. A. Holt, D. Leys, N. S. Scrutton, A. W. Munro, *Biochem. Soc. Trans.* **2005**, *33*, 747–753.

[15] a) C. F. Oliver, S. Modi, M. J. Sutcliffe, W. U. Primrose, L. Y. Lian, G. C. K. Roberts, *Biochemistry* **1997**, *36*, 1567–1572; b) P. Meinhold, M. W. Peters, A. Hartwick, A. R. Hernandez, F. H. Arnold, *Adv. Synth. Catal.* **2006**, *348*, 763–772; c) J. C. Lewis, F. H. Arnold, *Chimia* **2009**, *63*, 309–312; d) A. B. Carmichael, L. L. Wong, *Eur. J. Biochem.* **2001**, *268*, 3117–3125.

[16] a) S. Picataggio, T. Rohrer, K. Deanda, D. Lanning, R. Reynolds, J. Mielenz, L. D. Eirich, *Bio-Technology* **1992**, *10*, 894–898; b) W. H. Lu, J. E. Ness, W. C. Xie, X. Y. Zhang, J. Minshull, R. A. Gross, *J. Am. Chem. Soc.* **2010**, *132*, 15451–15455.

[17] a) J. M. Lebeault, E. T. Lode, M. J. Coon, *Biochem. Biophys. Res. Commun.* **1971**, *42*, 413–419; b) D. Sanglard, O. Käppeli, A. Fiechter, *J. Bacteriol.* **1984**, *157*, 297–302.

[18] M. Kusunose, M. J. Coon, E. Kusunose, *J. Biol. Chem.* **1964**, *239*, 1374–1380.

[19] G. Eggink, R. G. Lageveen, B. Altenburg, B. Witholt, *J. Biol. Chem.* **1987**, *262*, 17712–17718.

[20] E. J. McKenna, M. J. Coon, *J. Biol. Chem.* **1970**, *245*, 3882–3889.

[21] a) S. Benson, M. Fennewald, J. Shapiro, C. Huettner, *J. Bacteriol.* **1977**, *132*, 614–621; b) J. A. Peterson, D. Basu, M. J. Coon, *J. Biol. Chem.* **1966**, *241*, 5162–5164.

[22] J. B. van Beilen, J. Kingma, B. Witholt, *Enzyme Microb. Technol.* **1994**, *16*, 904–911.

[23] A. Schmid, J. S. Dordick, B. Hauer, A. Kiener, M. Wubbolts, B. Witholt, *Nature* **2001**, *409*, 258–268.

[24] O. Favre-Bulle, B. Witholt, *Enzyme Microb. Technol.* **1992**, *14*, 931–937.

[25] J. B. van Beilen, G. Eggink, H. Enequist, R. Bos, B. Witholt, *Mol. Microbiol.* **1992**, *6*, 3121–3136.

[26] C. Grant, J. M. Woodley, F. Baganz, *Enzyme Microb. Technol.* **2011**, *48*, 480–486.

[27] a) B. Witholt, M. J. de Smet, J. Kingma, J. B. van Beilen, M. Kok, R. G. Lageveen, G. Eggink, *Trends Biotechnol.* **1990**, *8*, 46–52; b) O. Favre-Bulle, T. Schouten, J. Kingma, B. Witholt, *Bio-Technology* **1991**, *9*, 367–371; c) M. G. Wubbolts, O. Favre-Bulle, B. Witholt, *Biotechnol. Bioeng.* **1996**, *52*, 301–308; d) A. Bosetti, J. B. Van Beilen, H. Preusting, R. G. Lageveen, B. Witholt, *Enzyme Microb. Technol.* **1992**, *14*, 702–708.

[28] a) B. G. Fox, Y. Liu, J. E. Dege, J. D. Lipscomb, *J. Biol. Chem.* **1991**, *266*, 540–550; b) W. A. Froland, K. K. Andersson, S. K. Lee, Y. Liu, J. D. Lipscomb, *J. Biol. Chem.* **1992**, *267*, 17588–17597.

[29] A. Perry, L. Y. Lian, N. S. Scrutton, *Biochem. J.* **2001**, *354*, 89–98.

[30] B. Bühler, J. B. Park, L. M. Blank, A. Schmid, *Appl. Environ. Microbiol.* **2008**, *74*, 1436–1446.

[31] J. B. van Beilen, T. H. M. Smits, F. F. Roos, T. Brunner, S. B. Balada, M. Rothlisberger, B. Witholt, *J. Bacteriol.* **2005**, *187*, 85–91.

[32] K. Lee, *J. Bacteriol.* **1999**, *181*, 2719–2725.

[33] a) L. Leive, *Ann. N. Y. Acad. Sci.* **1974**, *235*, 109–129; b) H. Nikaido, M. Vaara, *Microbiol. Rev.* **1985**, *49*, 1–32.

[34] S. D. Doig, H. Simpson, V. Alphand, R. Furstoss, J. M. Woodley, *Enzyme Microb. Technol.* **2003**, *32*, 347–355.

[35] J. B. Park, B. Bühler, T. Habicher, B. Hauer, S. Panke, B. Witholt, A. Schmid, *Biotechnol. Bioeng.* **2006**, *95*, 501–512.

[36] B. Bühler, B. Witholt, B. Hauer, A. Schmid, *Appl. Environ. Microbiol.* **2002**, *68*, 560–568.

[37] D. Meyer, B. Witholt, A. Schmid, *Appl. Environ. Microbiol.* **2005**, *71*, 6624–6632.

[38] M. Suzuki, T. Hayakawa, J. P. Shaw, M. Rekik, S. Harayama, *J. Bacteriol.* **1991**, *173*, 1690–1695.

[39] B. Bühler, A. Schmid, B. Hauer, B. Witholt, *J. Biol. Chem.* **2000**, *275*, 10085–10092.

[40] a) P. Goswami, H. D. Singh, *Biotechnol. Bioeng.* **1991**, *37*, 1–11; b) M. Rosenberg, E. Rosenberg, *J. Bacteriol.* **1981**, *148*, 51–57.

[41] J. Sambrook, D. W. Russell, *Molecular cloning – A laboratory manual*, Cold Spring Harbor Laboratory Press, Cold Spring Harbor (NY), **2001**.

[42] S. Panke, V. de Lorenzo, A. Kaiser, B. Witholt, M. G. Wubbolts, *Appl. Environ. Microbiol.* **1999**, *65*, 5619–5623.

[43] B. Bühler, I. Bollhalder, B. Hauer, B. Witholt, A. Schmid, *Biotechnol. Bioeng.* **2003**, *81*, 683–694.

[44] D. Hanahan, *J. Mol. Biol.* **1983**, *166*, 557–580.

[45] B. J. Bachmann, *Derivatisations and genotypes of some mutant derivatives of Escherichia coli K-12*, in: *Escherichia coli and Salmonella typhimurium – Cellular and molecualar biology*, (Ed.: C. F. Neidhardt), American Society for Microbiology, Washington, DC, Vol. 2, **1987**, pp 1190–1219.

[46] T. H. M. Smits, M. A. Seeger, B. Witholt, J. B. van Beilen, *Plasmid* **2001**, *46*, 16–24.

[47] H. van Heerikhuizen, E. Kwak, E. F. J. van Bruggen, B. Witholt, *Biochim. Biophys. Acta* **1975**, *413*, 177–191.

[48] M. Nieboer, J. Kingma, B. Witholt, *Mol. Microbiol.* **1993**, *8*, 1039–1051.

[49] U. K. Laemmli, *Nature* **1970**, *227*, 680–685.